*Inorg. Chem.* **2006**, *45*, 2075–2082


# Substituent Effects on Nitrosyl Iron Corrole Complexes Fe($Ar_3C$)(NO)

**Crisjoe A. Joseph, Matthew S. Lee,[1] Alexei V. Iretskii, Guang Wu, and Peter C. Ford***

*Department of Chemistry and Biochemistry, University of California, Santa Barbara, California 93106-9510*

Received November 11, 2005

A series of nitrosyl tris(5,10,15-aryl)corrolate complexes of iron(III) Fe($Ar_3C$)(NO) with different substituents on the aryl groups have been prepared, and certain spectroscopic and reaction properties were compared. The cyclic voltammetric analysis of the various Fe($Ar_3C$)(NO) complexes demonstrated that both the one-electron oxidation and one-electron reduction potentials respond in systematic and nearly identical trends relative to the electron-donor properties of the substituents. A similar pattern was seen in the nitrosyl stretching frequency, $\nu_{NO}$, which modestly decreased with the stronger donor substituents. Flash photolysis of Fe($Ar_3C$)(NO) solutions in toluene leads to NO dissociation followed by rapid [NO]-dependent decay of the transients formed (presumably Fe($Ar_3C$)) to regenerate the original spectra. As was seen in an earlier flash photolysis study of Fe(TNPC)(NO) ($TNPC^{3-}$ = 5,10,15-tris(4-nitro-phenyl)corrolate; Joseph, C.; Ford, P. C. *J. Am. Chem. Soc.* **2005**, *127*, 6737–6743), the second-order rate constants, $k_{NO}$, are all much faster ((1–9) $\times$ $10^8$ $M^{-1}$ $s^{-1}$ at 298 K) than those for analogous iron(III) complexes of porphyrins. However, on a more microscopic level there is no obvious pattern in these rates with respect to the donor properties of the aryl ring substituents. The high reactivity of the ferric triarylcorrolates with NO data is interpreted in terms of the strongly electron-donating character of the $Ar_3C^{3-}$ ligand and the quartet electronic configuration of the Fe($Ar_3C$) intermediate.

## Introduction

The metal complexes of non-porphyrin polypyrrole macrocycles are proving to have a very diverse chemistry including intriguing possibilities in areas ranging from catalysis to pharmaceuticals.[2,3] The interest in such systems is further enhanced by comparisons to the much more extensively investigated metallo porphyrinato complexes.[4] One such macrocycle is based on corrole, a "contracted porphyrin"[2] (shown below), which differs from its porphine analogue by having one less meso methine carbon, a skeletal perturbation that has a marked impact on its ligand properties.[3,5,6] The most obvious difference is that corrole and its derivatives have three ionizable N−H protons; thus, when coordinated to metal centers, the corrolate ligand is trianionic ($C^{3-}$), while the analogous porphyrinato ligand is dianionic ($P^{2-}$). The higher ionic charge and the smaller cavity of the corrolate macrocycle tends to stabilize metals in higher oxidation states, and tri- and tetravalent metal complexes are common.[7] The corrolates are receiving renewed interest as ligands because of improved synthetic procedures of the *meso*-aryl free-base corroles.[8]

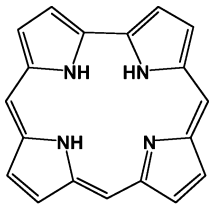


**corrole**

Nitric oxide has an established repertoire in mammalian biology with well-known roles in the cardiovascular, neurological, and immune response systems,[9] and much of this biochemistry involves the interactions between NO and metal centers.[10] The photochemical reactions of metal nitrosyls

* To whom correspondence should be addressed. E-mail: ford@chem.ucsb.edu.

(1) Taken in part from the M.S. thesis of M. S. Lee, University of California, Santa Barbara, CA 2005.

(2) Sessler, J. L.; Weghorn, S. J. In *Expanded, Contracted & Isomeric Porphyrins*; Baldwin, J. E., Ed.; Tetrahedron Organic Chemistry Series, Vol. 18; Pergamon: New York, 1997; pp 11−120.

(3) (a) Kadish, K. M.; Fremond, L.; Ou, Z.; Shao, J.; Shi, C.; Anson, F. C.; Burdet, F.; Gros, C. P.; Barbe, J.-M.; Guilard, R. *J. Am. Chem. Soc.* **2005**, *127*, 5625−5631. (b) Mohammed, A.; Gross, Z. *J. Am. Chem. Soc.* **2005**, *127*, 2883−2887. (c) Edwards, N. Y.; Eikey, R. A.; Loring, M. I.; Abu-Omar, M. M. *Inorg. Chem.* **2005**, *44*, 3700−3708. (d) Collman, J. P.; Decreau, R. A. *Organic Lett.* **2005**, *7*, 975−978. (e) Gryko, D. T.; Fox, J. P.; Goldberg, D. P. *J. Porphyrins Phthalocyanines* **2004**, *8*, 1091−1105.

(4) (a) *The Porphyrin Handbook*; Kadish, K. M., Smith, K. M., Guilard, R., Eds.; Academic Press: New York, 1959−2003; Vol. 1−20. (b) Wyllie, G. R. A.; Scheidt, W. R. *Chem. Rev.* **2002**, *102*, 1067−1090.

10.1021/ic051956j CCC: $33.50 
Published on Web 02/09/2006

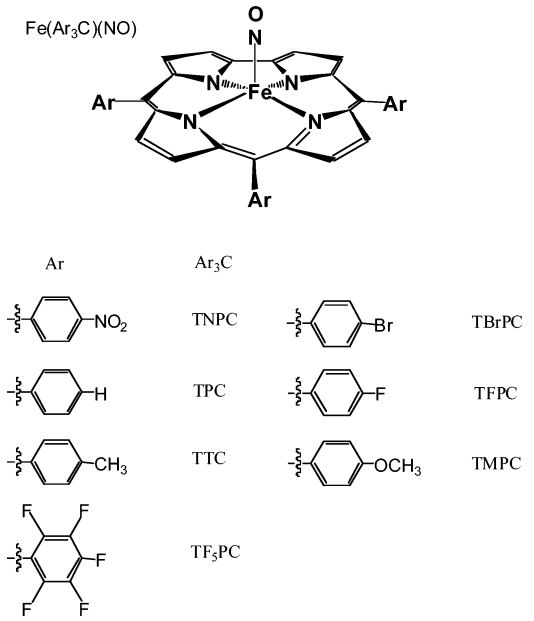


**Figure 1.** $Fe(Ar_3C)(NO)$ with labels corresponding to the respective $Ar_3C^{3-}$ ligands.

have shown promise in the development of strategies for the therapeutic delivery of NO to specific tissue sites.[11] These parallel themes have drawn the attention of this laboratory[12] and others[13] who have been concerned with systematic elucidation of the mechanisms of NO reactions with metal centers including those of various ferri- and ferro-heme proteins and models. One goal of probing the analogous reactions of ferric corrole complexes is to provide better insight into the parameters defining the reactivities of analogous heme models. Described here are the investigations of several nitrosyl complexes of iron(III) tris(5,10,15-aryl)corrolates $Fe(Ar_3C)(NO)$[14] (Figure 1) initiated with the goal of probing the effects of aryl group substituents.

## Experimental Section

**Materials.** Spectrochemical grade toluene (Burdick & Jackson) was distilled from sodium. Dichloromethane for the electrochemical measurements was distilled from calcium hydride and stored over sieves. Pyrrole and benzaldehyde derivatives (Aldrich) were distilled and stored in the dark, under nitrogen, in the refrigerator. Tetrabutylammonium hexafluorophosphate (TBAHP) was recrystallized from methanol. Ferrocene used as an electrochemical internal standard was purified by sublimation. Other organic compounds (Aldrich) were used as purchased without further purification. Nitric oxide (99%, Aire Liquide) was purified by passage through a stainless steel column containing Ascarite II (Thomas Scientific), attached via an O-ring seal (Viton) to a greaseless vacuum line.

**Electrochemistry.** Cyclic voltammetry experiments were performed using a BAS 100A Electrochemical Analyzer potentiostat with a conventional three-electrode system: a glassy carbon disk working electrode, a platinum wire counter electrode, and an Ag/AgCl reference electrode. All measurements were conducted in $CH_2Cl_2$ using TBAHP as a supporting electrolyte. The solutions were entrained with argon prior to each run, and an Ar atmosphere was maintained over the solutions during the electrochemical measurements. Ferrocene was used as an internal standard.

**Computations.** The equilibrium geometry of the Fe(C)(NO) complex was optimized at the B3LYP/LACVP* level as a singlet state without any symmetry constraints and represents the gas-phase structure (Spartan04, Wavefunction, Inc.).

**Flash Photolysis Experiments.** Solutions of known concentrations of NO and $Fe(Ar_3C)(NO)$ were prepared by vacuum transfer techniques in all-glass vacuum lines using procedures designed to prevent contamination with other $NO_x$ impurities. The "pump-probe" flash photolysis apparatus has been described previously.[15,16]

(5) (a) Vogel, E.; Will, S.; Tilling, A. S.; Neumann, L.; Lex, J.; Bill, E.; Trautwein, A. X.; Wieghardt, K. *Angew. Chem., Int. Ed. Engl.* **1994**, *33*, 731−735. (b) Autret, M.; Will, S.; Caemelbecke, E. V.; Lex, J.; Gisselbrecht, J.-P.; Gross, M.; Vogel, E.; Kadish, K. M. *J. Am. Chem. Soc.* **1994**, *116*, 9141−9149. (c) Caemelbecke, E. V.; Will, S.; Autret, M.; Adamian, V. A.; Lex, J.; Gisselbrecht, J.-P.; Gross, M.; Vogel, E.; Kadish, K. M. *Inorg. Chem.* **1996**, *35*, 184−192.

(6) (a) Simkhovich, L.; Goldberg, I.; Gross, Z. *Inorg. Chem.* **2002**, *41*, 5433−5439. (b) Gross, Z.; Galili, N.; Simkhovich, L.; Saltsman, I.; Botoshansky, M.; Blaser, D.; Boese, R.; Goldberg, I. *Org. Lett.* **1999**. (c) Meier-Callahan, A. E.; Di Bilio, A. J.; Simkhovich, L.; Mohammed, A.; Goldberg, I.; Gray, H. B.; Gross, Z. *Inorg. Chem.* **2001**, *40*, 6788−6793. (d) Mohammed, A.; Gray, H. B.; Meier-Callahan, A. E.; Gross, Z. *J. Am. Chem. Soc.* **2003**, *125*, 1162−1163.

(7) (a) Steene, E.; Wondimagegn, T.; Ghosh, A. *J. Phys. Chem. B* **2001**, *105*, 11406−11413. (b) Cai, S.; Licoccia, S.; Walker, F. A. *Inorg. Chem.* **2001**, *40*, 5795−5798. (c) Ramdhanie, B.; Zakharov, L. N.; Rheingold, A. R.; Goldberg, D. P. *Inorg. Chem.* **2002**, *41*, 4105−4107.

(8) (a) Paolesse, R.; Nardis, S.; Sagone, F.; Khoury, R. G. *J. Org. Chem.* **2001**, *66*, 550−556. (b) Geier, G. R., III; Chick, J. F. B.; Callinan, J. B.; Reid, C. G.; Auguscinski, W. P. *J. Org. Chem.* **2004**, *69*, 4159.

(9) (a) *Nitric Oxide, Biology and Pathology*; Ignarro, L. J., Ed.; Academic Press: San Diego, 2000. (b) Richter-Addo, G. B.; Legzdins, P.; Burstyn, J. *Chem. Rev.* **2002**, *102*, 857−1270.

(10) (a) Traylor, T. G.; Sharma, V. S. *Biochemistry* **1992**, *31*, 2847. (b) Radi, R. *Chem. Res. Toxicol.* **1996**, *9*, 828. (c) Ford, P. C.; Laverman, L. E.; Lorkovic, I. M. *Adv. Inorg. Chem.* **2003**, *54*, 203−257.

(11) For examples, see: (a) Davies, K. M.; Wink, D. A.; Saavedra, J. E.; Keefer, L. K. *J. Am. Chem. Soc.* **2001**, *123*, 5473−5481. (b) *Methods in Nitric Oxide Research*; Feelisch, M., Stamler, J. S., Eds.; J. Wiley & Sons: West Sussex, England, 1996; Chapter 7, pp 71−115. (c) Bourassa, J.; DeGraff, W.; Kudo, S.; Wink, D. A.; Mitchell, J. B.; Ford, P. C. *J. Am. Chem. Soc.* **1997**, *119*, 2853−2862. (d) Namiki, S.; Arai, T.; Fujimori, K. *J. Am. Chem. Soc.* **1997**, *119*, 3840−3841. (e) Megson, I. L.; Webb, D. J. *Expert Opin. Invest. Drugs* **2002**, *11*, 587−601. (f) Wang, P. G.; Xian, M.; Tang, X.; Wu, X. Wen, Z.; Cai, T.; Janczuk, A. J. *Chem. Rev.* **2002**, *102*, 1091−1134.

(12) (a) Hoshino, M.; Ozawa, K.; Seki, H.; Ford, P. C. *J. Am. Chem. Soc.* **1993**, *115*, 9568−9575. (b) Hoshino, M.; Maeda, M.; Konishi, R.; Seki, H.; Ford, P. C. *J. Am. Chem. Soc.* **1996**, *118*, 5702−5707. (c) Laverman, L. E.; Hoshino, M.; Ford, P. C. *J. Am. Chem. Soc.* **1997**, *119*, 12663−12664. (d) Lorkovic, I. M.; Ford, P. C. *Inorg. Chem.* **1999**, *38*, 1467−1473. (e) Lorkovic, I. M.; Ford, P. C. *J. Am. Chem. Soc.* **2000**, *122*, 6516−6517. (f) Laverman, L. E.; Wanat, A.; Oszajca, J.; Stochel, G.; Ford, P. C.; van Eldik, R. *J. Am. Chem. Soc.* **2001**, *123*, 285−293. (g) Laverman, L. E.; Ford, P. C. *J. Am. Chem. Soc.* **2001**, *123*, 11614−11622. (h) Kurtikyan, T. S.; Martirosyan, G. G.; Lorkovic, I. M.; Ford, P. C. *J. Am. Chem. Soc.* **2002**, *124*, 10124−10129. (i) Fernandez, B. O.; Ford, P. C. *J. Am. Chem. Soc.* **2003**, *125*, 10510−10511. (j) Patterson, J C.; Lorkovic, I. M.; Ford, P. C. *Inorg. Chem.* **2003**, *42*, 4902−4908. (k) Fernandez, B. O.; Lorkovic, I. M.; Ford, P. C. *Inorg. Chem.* **2004**, *43*, 5393−5402.

(13) For example, see: (a) Moore, E. G.; Gibson, Q. H. *J. Biol. Chem.* **1976**, *251*, 2788. (b) Rose, E. J.; Hoffman, B. M. *J. Am. Chem. Soc.* **1983**, *105*, 2866. (c) Hoshino, M.; Laverman, L.; Ford, P. C. *Coord. Chem. Rev.* **1999**, *187*, 75−102 and references therein. (d) Cheng, L.; Richter-Addo, G. B. Chpt. 33 in Vol. 4 of reference 4a. (e) Franke, A.; Stochel, G.; Jung, C.; van Eldik, R. *J. Am. Chem. Soc.* **2004**, *126*, 4181−4191.

(14) (a) The interaction between a metal center and a coordinated NO is often accompanied by considerable charge transfer which often characterizes the structure and reactivity for the M−NO unit, for example it is common to represent the bonding between Fe(III) and NO as an $Fe^{II}(NO^+)$ complex. However, it should be emphasized that these are delocalized systems and perhaps better represented using the Feltham/Enemark designation[14b] $\{MNO\}^n$, where $n$ is the sum of the metal d electrons and NO $\pi^*$ electrons ($\{FeNO\}^6$ in the case of Fe(III) and NO). In the present case, $Fe(Ar_3C)(NO)$ will generally be referred to as Fe(III) complexes of NO without intending any conclusion about the charge distribution. (b) Enemark, J. H.; Feltham, R. D. *Coord. Chem. Rev.* **1974**, *13*, 339−406.

The excitation source ("pump") was a Continuum NY-61 Nd:YAG pulse laser operating in the frequency-tripled (355 nm) or -doubled (532 nm) mode with a pulse energy of ~10 mJ. Transient absorption changes were monitored with a monochromatic probe light beam focused into the sample (at a right angle to the excitation beam) through a double-grating monochromator (SPEX model 1680) and onto a photomultiplier tube (RCA IP28). The temporal response (25 shot averages) was recorded using a digital oscilloscope (Tektronix TDS 540) linked to a desktop computer. Plots of intensity versus time were converted to absorbance, and these curves were fit using Igor Pro Carbon software (Wavemetrics).

**Spectroscopic Measurements.** UV−vis spectra were recorded using either a Hewlett-Packard model 8452A diode array or a Shimadzu UV-2401PC spectrophotometer. The solutions were prepared and contained in a custom-made glass flask of measured volume fused to a 1 cm path length quartz cuvette and equipped with a coldfinger and a high-vacuum stopcock for connection to a vacuum line. Infrared spectra were recorded using a Jasco FT/IR-4600 Plus Fourier transform infrared spectrometer with a Jasco Pike Miracle ATR accessory. All spectra were acquired as an average of 32 scans with a 1 cm$^{-1}$ resolution. Infrared spectra were also recorded on a Bio-Rad FTS-60 SPC 3200 FTIR spectrophotometer. Mass spectra were obtained using a VG Fisons Platform II single quadrupole mass spectrometer with an electrospray ionization source run with a Fisons Masslinks data system. NMR spectra were obtained on Varian 200 and 400 MHz spectrometers.

**Syntheses.** The free base tris(aryl) corroles ($H_3Ar_3C$), 5,10,15-tris(penta-fluorophenyl)corrole ($H_3TF_5PC$), 5,10,15-tris(4-nitrophenyl)corrole (**(**$H_3$TNPC), 5,10,15-tris(4-bromophenyl)corrole (**(**$H_3$TBrPC), 5,10,15-tris(4-fluorophenyl)corrole (**(**$H_3$TFPC), 5,10,15-tris(phenyl)corrole ($H_3$TPC), 5,10,15-tris(4-tolyl)corrole ($H_3$TTC), and 5,10,15-tris(4-methoxy-phenyl)corrole (**(**$H_3$TMOPC), were prepared via the reactions of freshly distilled pyrrole (Aldrich) with the appropriate substituted benzaldehyde in refluxing acetic acid according to published procedures for the synthesis of corroles.[7a] These compounds were purified by chromatography of the crude reaction mixtures on an initial silica column using $CH_2Cl_2$ as the elutant and then on a second silica column using $CH_2Cl_2$/hexanes (10:1) as the elutant. If impurities still persisted, additional chromatography was carried out. The ligands were characterized and shown to be pure by $^1$HNMR, UV−vis, and mass spectroscopic techniques. Overall yields were in the 3−10% range, while the respective tetra(aryl) porphyrins ($H_2Ar_4P$) were formed as "side-products" in varying yields.

The iron complexes Fe(Ar$_3$C)(NO) were formed via procedures reported previously for the preparation of other Fe(Ar$_3$C)(NO) complexes.[6a] A mixture of $FeCl_2$·$4H_2O$ (1.5 mmol) and the free base corrole (75 $\mu$mol) in pyridine/methanol (1:2) was refluxed for 3 h under dinitrogen, after which a 1.0 mL aliquot of saturated aqueous $NaNO_2$ was added to the hot solution, and the system was refluxed for an additional 30 min. The solution was then cooled to 0 °C, and the resulting solid was collected by filtration and washed with water. This solid product was dissolved in dichloromethane and purified by chromatography on an alumina column (Brockman Activity III) using $CH_2Cl_2$/hexane (1:3) as the elutant. If impurities still persisted, this procedure was repeated. Overall yields averaged 75−85%.

**Table 1.** Crystal Data and Structure Refinement for Fe(TTC)(NO) (TTC = the 5,10,15-tris(4-tolyl)corrolato trianion) and for Fe(TMOPC)(NO) (TMOPC = the 5,10,15-tris(4-methoxyphenyl)corrolato trianion)

| | Fe(TTC)(NO) | Fe(TMOPC)(NO) |
|---|---|---|
| empirical formula | $C_{46}H_{35}FeN_5O$ | $C_{46}H_{35}FeN_5O_4$ |
| fw | 729.64 | 777.64 |
| temp | 118(1) K | 120(1) K |
| wavelength | 0.71073 Å | 0.71073 Å |
| cryst syst, space group | triclinic, $P\bar{1}$ | triclinic, $P\bar{1}$ |
| unit cell dimensions | $a$ = 10.652(1) Å | $a$ = 10.547(4) Å |
| | $b$ = 10.923(1) Å | $b$ = 11.047(5) Å |
| | $c$ = 15.285(2) Å | $c$ = 15.916(7) Å |
| | $\alpha$ = 87.514(2)° | $\alpha$ = 101.196(7)° |
| | $\beta$ = 85.987(2)° | $\beta$ = 92.972(7)° |
| | $\gamma$ = 84.216(2)° | $\gamma$ = 90.164(7)° |
| vol | 1763.9(4) Å$^3$ | 1816.5(13) Å$^3$ |
| $Z$, density$_{calcd}$ | 2, 1.374 Mg/m$^3$ | 2, 1.422 Mg/m$^3$ |
| abs coeff | 0.473 mm$^{-1}$ | 0.470 mm$^{-1}$ |
| $F$(000) | 760 | 808 |
| cryst size | 0.3 × 0.3 × 0.1 m | 0.15 × 0.10 × 0.04 mm |
| $\theta$ range for data collection | 1.34−28.15° | 1.31−26.55° |
| limiting indices | $-14 \le h \le 13$ | $-13 \le h \le 13$ |
| | $-14 \le k \le 13$ | $-13 \le k \le 13$ |
| | $-19 \le l \le 19$ | $-19 \le l \le 19$ |
| reflns collected/unique | 15172/7541 [$R$(int) = 0.0264] | 13739/7189 [$R$(int) = 0.0685] |
| completeness to $\theta$ = 28.15 | 87.10% | 95.2% |
| abs correction | SADABS | SADABS |
| refinement method | full-matrix least-squares on $F^2$ | full-matrix least-squares on $F^2$ |
| data/restraints/params | 7541/0/618 | 7189/0/646 |
| GOF on $F^2$ | 1.036 | 1.110 |
| final R indices [$I > 2\sigma(I)$] | R1 = 0.0431 wR2 = 0.1105 | R1 = 0.0708 wR2 = 0.1289 |
| R indices (all data) | R1 = 0.0612 wR2 = 0.1190 | R1 = 0.1484 wR2 = 0.1461 |
| largest diff. peak and hole | 0.666 and −0.589 Å$^3$ | 0.781 and −1.008 Å$^3$ |

**[Fe(TF$_5$PC)(NO)] (1) (TF$_5$PC$^{3-}$ = 5,10,15-Tris(pentafluorophenyl)corrolate).**[6a] ESI-MS: $m/z$ 848 (M − NO)$^+$. UV−vis: $CH_2Cl_2$ $\lambda_{max}$ 379 (1.00), 538 nm (0.15).[17] IR: $\nu_{NO}$ 1801 cm$^{-1}$ (thin film).

**[Fe(TNPC)(NO)] (2) (TNPC$^{3-}$ = 5,10,15-Tris(4-nitrophenyl)-corrolate).** $^1$HNMR ($CDCl_3$): $\delta$ 7.37 (d, 2H, $J$ = 5 Hz), 7.55 (d, 2H, $J$ = 5 Hz), 7.76 (d, 2H, $J$ = 4 Hz), 7.85 (dd, 1H, $J$ = 8 Hz), 7.90 (dd, 1H, $J$ = 8 Hz), 8.04 (d, 4H, $J$ = 8 Hz), 8.11 (d, 2H, $J$ = 4 Hz), 8.45 (dd, 2H, $J$ = 8 Hz), 8.51 (d, 4H, $J$ = 8 Hz). MS(FAB): $m/z$ 744 (M$^+$), 714 (M$^+$ − NO). IR: $\nu_{NO}$ 1772 (thin film), 1778 (KBr), 1785 cm$^{-1}$ ($CHCl_3$). UV−vis: toluene $\lambda_{max}$ 392 ($\epsilon$ = 6.0 × 10$^4$ M$^{-1}$ cm$^{-1}$), 538 nm (7.8 × 10$^3$ M$^{-1}$ cm$^{-1}$); $CH_2Cl_2$ $\lambda_{max}$ 271 ($\epsilon$ = 3.2 × 10$^4$ M$^{-1}$ cm$^{-1}$), 382 (6.5 × 10$^4$ M$^{-1}$ cm$^{-1}$), 541 nm (1.15 × 10$^4$ M$^{-1}$ cm$^{-1}$).

**[Fe(TBrPC)(NO)] (3) (TBrPC$^{3-}$ = 5,10,15-Tris(4-bromophenyl)-corrolate).** ESI-MS: $m/z$ 845 (M)$^+$, 815 (M − NO)$^+$. IR: $\nu_{NO}$ 1767 cm$^{-1}$ (thin film). UV−vis: $CH_2Cl_2$ $\lambda_{max}$ 397 (1.00), 535 nm (0.12).[17]

**[Fe(TFPC)(NO)] (4) (TFPC$^{3-}$ = 5,10,15-Tris(4-fluorophenyl)-corrolate).** $^1$H NMR ($CDCl_3$): $\delta$ 7.30 (m,10H), 7.47 (d, 2H, $J$ = 5), 7.64 (m, 6H), 7.82 (d, 2H, $J$ = 5). ESI-MS: $m/z$ 663 (M)$^+$, 633 (M − NO)$^+$. IR: $\nu_{NO}$ 1767 cm$^{-1}$ (thin film). UV−vis: $CH_2Cl_2$ $\lambda_{max}$ 390 (1.00), 532 nm (0.067).[17]

**[Fe(TPC)(NO)] (5) (TPC$^{3-}$ = 5,10,15-Tris(phenyl)corrolate).** $^1$H NMR ($CDCl_3$): $\delta$ 7.39 (d, 2H, $J$ = 5 Hz), 7.59 (m, 9H), 7.76 (d, 6H, $J$ = 4 Hz), 7.86 (dd, 4H, $J$ = 8 Hz), 7.96 (d, 2H, $J$ = 5 Hz). ESI-MS: $m/z$ 609 (M$^+$), 579(M$^+$ − NO). IR: $\nu_{NO}$ 1767 (thin film), 1766 cm$^{-1}$ (KBr). UV−vis: $CH_2Cl_2$ $\lambda_{max}$ 390 ($\epsilon$ = 7.1 × 10$^4$ M$^{-1}$ cm$^{-1}$), 534 nm (8.1 × 10$^3$ M$^{-1}$ cm$^{-1}$).

(15) Lorkovic, I. M.; Miranda, K. M.; Lee, B.; Bernhard, S.; Schoonover, J. R.; Ford, P. C. *J. Am. Chem. Soc.* **1998**, *120*, 11674−11683.
(16) Joseph, C. A.; Ford, P. C. *J. Am. Chem. Soc.* **2005**, *127*, 6737−6743.
(17) For those cases where the extinction coefficients of isolated Fe(Ar$_3$C)(NO) complexes were not determined accurately, the relative intensities of the absorption bands are reported as normalized to the intensity of the Soret band at ~390 nm. Similar to porphyrinato analogues, each of these compounds displayed a very strong Soret band with an extinction coefficient of nearly 10$^5$ M$^{-1}$ cm$^{-1}$ and a Q-type band at ~540 nm which was about a factor of 8 less intense.

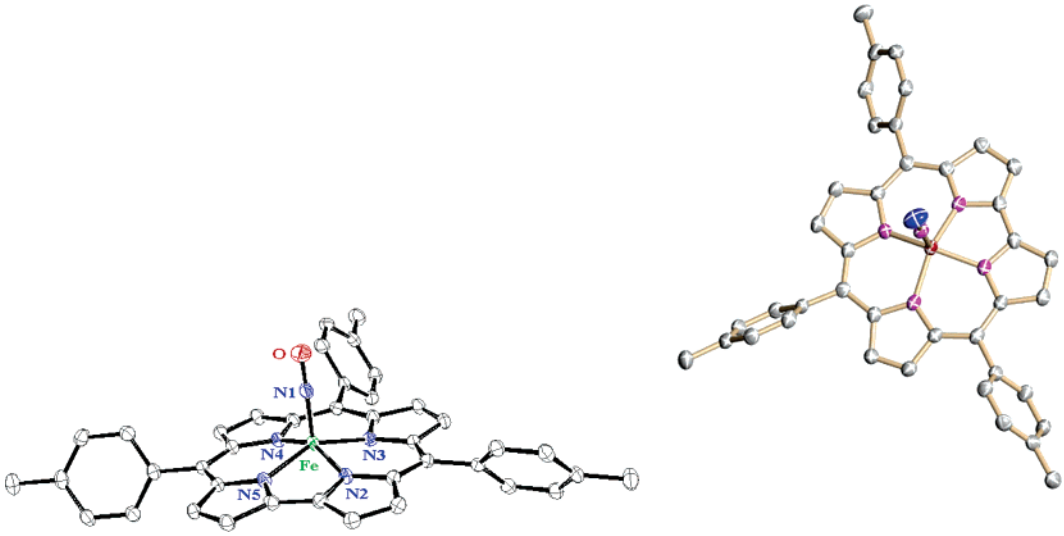


**Figure 2.** ORTEP diagram of Fe(TTC)(NO) (**6**) (two views). Hydrogens, solvent, and selected labels are omitted for clarity.

**Table 2.** Selected Crystallographic Data for the Fe(TMOPC)(NO) and Fe(TTC)(NO) Complexes

| | Fe(TMOPC)(NO) (**7**) | Fe(TTC)(NO) (**6**) |
|---|---|---|
| | bond lengths (Å) | |
| Fe−N1 | 1.702(4) | 1.645(2) |
| Fe−N2 | 1.890(4) | 1.897(2) |
| Fe−N3 | 1.922(4) | 1.934(2) |
| Fe−N4 | 1.900(4) | 1.923(2) |
| Fe−N5 | 1.878(4) | 1.899(2) |
| N1−O | 1.076(4) | 1.162(2) |
| | deviation from ideal plane (Å)[a] | |
| N2 | 0.035(2) | 0.036(1) |
| N3 | −0.031(2) | −0.0309(8) |
| N4 | 0.031(2) | 0.0310(8) |
| N5 | −0.036(2) | −0.036(1) |
| Fe | 0.449(2) | 0.455(1) |
| | angles (deg) | |
| Fe−N1−O | 172.0(4) | 177.1(2) |
| N2−Fe−N3 | 87.5(2) | 87.65(8) |
| N3−Fe−N4 | 92.6(2) | 92.85(8) |
| N4−Fe−N5 | 87.7(2) | 87.36(8) |
| N5−Fe−N2 | 79.4(2) | 79.19(8) |

[a] Calculated least squares plane using N2, N3, N4, and N5 ($x$, $y$, $z$ in crystal coordinates). Fe(TMOPC)(NO): $(4.84 \pm 0.01)x + (6.55 \pm 0.01)y + (8.08 \pm 0.02)z = 11.527 \pm 0.008$. Fe(TTC)(NO): $(4.600 \pm 0.007)x + (7.656 \pm 0.005)y + (8.523 \pm 0.009)z = 2.36 \pm 0.01$).

**[Fe(TTC)(NO)] (6) (TTC$^{3-}$ = 5,10,15-Tris(4-tolyl)corrolate).** $^1$H NMR ($CDCl_3$): $\delta$ 2.54 (bs, 9H), 7.41(m,10H), 7.58 (d, 2H, $J$ = 5 Hz), 7.75 (m,6H), 7.93 (d, 2H, $J$ = 5 Hz). ESI-MS: $m/z$ 651 ($M^+$), 621($M^+$ − NO ). IR: $\nu_{NO}$ 1767 (thin film), 1762 cm$^{-1}$ (KBr). UV−vis: $CH_2Cl_2$ $\lambda_{max}$ 400 (1.00), 532 nm (0.125).[17] An X-ray crystal structure of this compound was determined.

**[Fe(TMOPC)(NO)] (7) (TMOPC$^{3-}$ = 5,10,15-Tris(4-methoxyphenyl)corrolate).** $^1$H NMR ($CDCl_3$): $\delta$ 3.97 (bs, 9H), 7.141 (m, 6H), 7.44 (d, 2H, $J$ = 5 Hz), 7.60 (bd, 3H, $J$ = 5 Hz), 7.78 (m, 7H), 7.93 (d, 2H, $J$ = 5 Hz). ESI-MS: $m/z$ 699 $(M + H)^+$, 668 $(M + H - NO)^+$. IR: $\nu_{NO}$ 1761 cm$^{-1}$ (thin film). UV−vis: $CH_2Cl_2$ $\lambda_{max}$ 365 (0.49), 416 (1.00), 533 nm (0.15).[17] An X-ray crystal structure of this compound was determined.

**Crystal Growth and Structure Determination.** The crystal structures for Fe(TTC)(NO) **(6)** and Fe(TMOPC)NO **(7)** were determined (Table 1). Crystals of **6** and **7** were grown via slow vapor diffusion of pentane into a concentrated benzene solution. Single crystals were mounted on a glass fiber and transferred to a Bruker CCD platform diffractometer. The SMART program was used to determine the unit cell parameters and data collection (20 s/frame, 0.3°/frame for a sphere of diffraction data). Studies were carried out at low temperature. The raw frame data were processed using the SAINT program. The absorption correction was applied using the program SADABS. Subsequent calculations were carried out using the SHELXTL program.

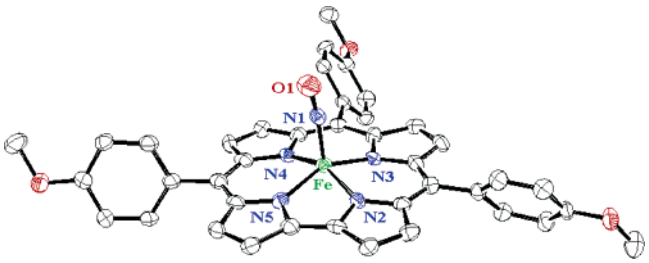


**Figure 3.** ORTEP diagram of Fe(TMOPC)(NO) (**7**). Hydrogens, solvent, and selected labels are omitted for clarity.

The structure was solved by direct methods and was refined on $F^2$ by full-matrix least-squares techniques. Hydrogen atoms were located from difference Fourier map. Relevant atomic coordinates, bond lengths, and bond angles are given in Table 2 and Supporting Information Tables S1a−f and S2a−f. The molecular structure of Fe(TTC)(NO) is shown in Figure 2, and the cell packing structure is shown in Supporting Information Figure S1. The molecular structure of Fe(TMOPC)(NO) is shown in Figure 3, and the cell packing structure is shown in Supporting Information Figure S2.

## Results and Discussion

**Structures.** The ORTEP diagrams for Fe(TTC)(NO) and Fe(TMOPC)(NO) (Figures 2 and 3) show the molecule adopting a distorted square pyramidal geometry about a 5-coordinate iron atom for both molecules. The four corrole nitrogens form a near ideal plane and the iron is displaced ∼0.45 Å above the plane (Δ) (Table 2). The square pyramid formed by the apical iron and four corrole nitrogens is somewhat distorted. The two Fe−N bonds forming one side of the pyramid (Fe−N2 and Fe−N5) are somewhat shorter (∼0.02 Å) than the other two, and the N2−Fe−N5 bond angle is more acute than the other three angles defining the square pyramid because of N2 and N5 being the nitrogens of the pyrrole rings linked without the methine bridge. The

**Table 3.** Comparison of Structural Data for Fe(TMOPC)(NO) and Fe(TTC)(NO) to Previously Determined Structures of Other Fe(C)(NO) and Several Porphyrinato Analogs

| complex | Fe−N$_{ring}$ (Å) | Fe−N$_{NO}$ (Å) | ∠FeNO (deg) | N−O (Å) | $D^a$ (Å) | $n_{NO}$ (cm$^{-1}$) | ref |
|---|---|---|---|---|---|---|---|
| Fe(TMOPC)(NO) | 1.898(4) | 1.702(4) | 172.0(4) | 1.076(4) | 0.449(2) | 1761[b] | *b* |
| Fe(TTC)(NO) | 1.913(2) | 1.645(2) | 177.1(2) | 1.162(2) | 0.455(1) | 1767[b] | *b* |
| Fe(TDCC)(NO) | 1.910(4) | 1.641(4) | 172.3(4) | 1.169(5) | 0.452(2) | 1783[c] | 6a |
| Fe(TF$_5$PC)(NO)[d] | 1.910(4), | 1.639, | 177.3, | 1.164, | 0.465 | 1790[c], | 6a |
| | 1.910(4) | 1.648(4) | 178.0(4) | 1.166(4) | 0.464(2) | 1801[b] | |
| Fe(OEC)(NO) | 1.909(3) | 1.631(3) | 176.9(3) | 1.171(4) | 0.470(1) | 1758[e] | 5b |
| Fe(OEC)(NO)$^+$ | 1.912(8) | 1.66(1) | 171.4(9) | 1.12(1) | 0.406(5) | 1809[e] | 5b |
| Fe(TPP)(NO)[f] | 2.001(3) | 1.717(7) | 149.2(6) | 1.12(1) | 0.211 | 1670[c] | 4b |
| Fe(TPP)(NO)(1-MeIm)[g] | 2.01(1) | 1.743(4) | 142.1(6) | 1.121(8) | 0.07 | 1625[c] | 4b |
| [Fe(OEP)(NO)]-[ClO]$_4$[h] | 1.994(5) | 1.653(1) | 173.2(1) | 1.140(2) | 0.32 | 1838[i] | 4b |
| [Fe(TPP)(NO)(HO-*i*-C$_5$H$_{11}$)]$^+$ | 2.013(3) | 1.776(5) | 177.1(7) | 0.925(6) | 0.05 | 1935[c] | 4b |

[a] Distance of iron atom from mean plane of the four pyrrole nitrogen atoms. [b] This work, IR taken as thin film. [c] IR taken as KBr Pellets. [d] There are two crystallographically independent corrole species reported in the unit cell. [e] IR taken as CsI pellet. [f] Eight-fold disorder of NO, TPP = tetraphenylporphyrinate. [g] Two positions of nitrosyl ligand observed. [h] Nonsolvated form, OEP = octaethylporphyrinate. [i] IR taken as Nujol mull.

Fe−N−O angles are nearly linear (177.1° and 172.0° for **6** and **7**, respectively) as expected for tetragonal {FeNO}$^6$ complexes, which are sometimes described as having Fe$^{II}$(NO$^+$) character.[14] In these contexts, the structures of **6** and **7** are in good agreement with those for the previously published iron nitrosyl corrolate complexes Fe(TF$_5$PC)(NO),[6a] Fe(TDCC)(NO)[6a] (TDCC = 5,10,15-tris-(2,6-dichlorophenyl)-corrolate), and Fe(OEC)(NO)[5b] (OEC = octaethylcorrolate). In all five, the iron is pentacoordinate and is displaced substantially ($\Delta$ = 0.41−0.47 Å) out of the corrolate N$_4$ plane, while ∠Fe−N−O is close to linear. In the crystal packing diagrams (Figures S1 and S2), adjacent Fe(Ar$_3$C)(NO) molecules in the unit cell are positioned back-to-back, with the corrole ligands noneclipsing but with the planes of the rings approximately parallel, being 3.635 and 3.582 Å apart, respectively. Solvent benzene in the crystals of **6** and **7** occupies the voids between the complexes. The ability to record $^1$HNMR spectra in solutions indicates that these compounds are diamagnetic.[14]

The two new and three previously published[5b,6a] Fe$^{III}$(C)(NO) structures are compared in Table 3 with several typical nitrosyl Fe(III) and Fe(II) ({FeNO}$^6$ and {FeNO},$^7$ respectively) porphyrinato complexes. The majority of the reported ferrous Fe(P)(NO) structures (P$^{2-}$ = porphyrinato) reported are pentacoordinate[4b] with the iron is displaced above the N$_4$ plane of the porphyrin ($\Delta$ = 0.21−0.32 Å) and an Fe−N−O angle in the range 139−149°. The less common six coordinate {FeNO}$^7$ complexes display very small $\Delta$ values (<0.1 Å) but similarly acute Fe−N−O angles (Table 3). Most of the nitrosyl complexes of the ferric porphyrinato complexes that have been structurally characterized are six-coordinate and usually have a very small value of $\Delta$ (<0.1 Å). Like the corrole analogues, these Fe(P)(X)(NO) complexes generally display near linear Fe−N−O angles, although exceptions are seen when X is a very strong $\sigma$ donor ligand such as the nitro ($NO_2^-$) or *p*-fluorophenyl anion.

The Fe(C)(NO) structures are most similar to the electronically analogous 5-coordinate [Fe(OEP)(NO)]$^+$ cation, also marked by considerable displacement of the iron above the porphyrin ring ($\Delta$ = 0.32 Å) and a nearly linear ∠Fe−N−O. For the former, $\Delta$ is much larger, consistent with the smaller size of the corrolate ring. This is evidenced by the distances between the nonadjacent nitrogens (N3−N5 or N2−N4), which for the corrolates, 3.70 ± 0.01 Å, is considerably shorter than that found for ferrous porphyrin nitrosyls (4.00 ± 0.02 Å) or the ferric analogues (3.97 ± 0.05 Å).[18] Another difference is that the iron to corrolate ring nitrogen bond lengths (1.88−1.93 Å for **6** and **7**) are significantly shorter than those found for [Fe(OEP)(NO)]$^+$ (av 1.99 Å) and other 5- or 6-coordinate {FeNO}$^6$ and {FeNO}$^7$ porphyrinato complexes (1.95−2.01 Å) because of the greater charge and smaller cavity of the C$^{3-}$ ligands.

The Fe−NO bond in **6** is 1.645 Å, which is shorter than those found in the Fe$^{II}$(P)(NO) complexes (1.691−1.743 Å) and similar to those found in the Fe$^{III}$(P)(NO) compounds (1.627−1.728 Å).[19] However, the N−O bond (1.162 Å) for **6** is longer compared to those found in Fe$^{II}$(P)(NO) and Fe$^{III}$(P)(NO) (1.112−1.167 Å).[19] These measurements of the Fe−N−O moiety are in line with those of previously reported iron nitrosyl corroles (Table 3). However, the N−O and Fe−N distances found in Fe(TMOPC)(NO) are inexplicably skewed. The N−O distance is substantially smaller and the Fe−NO distance is longer than the respective values observed in the other Fe(C)NO complexes. Re-examination of the crystal data showed no erroneous peaks around the FeNO unit, and the X-ray scattering is quite clean. Furthermore, there is no obvious interaction between the NO and methoxy oxygen atoms of another corrolate complex. When the crystal structure was solved at a lower symmetry, the correlation was poorer and the anomalous distances persisted. The only substantial difference between **7** and **6** lies in the packing structures**,** the molecules are more closely packed in **7** than in **6**. Why this might lead to a skewing of the Fe−N−O moiety is unknown.

**Electrochemical Studies.** The cyclic voltammogram of Fe(TFPC)(NO) in $CH_2Cl_2$ containing 0.1 M TBAHP is shown in Figure 4. The octaethylcorrolate complex Fe(OEC)-

(18) (a) Distances for ferrous nitrosyl porphyrins were calculated on the basis of the data for Fe(TPP)(NO)[18b] and Fe(TPP)(NO)(1-MeIm).[18c] (b) Scheidt, W. R.; Frisse, M. E. *J. Am. Chem. Soc.* **1975**, *97*, 17−21. (c) Scheidt, W. R.; Piciulo, P. L. *J. Am. Chem. Soc.* **1976**, *98*, 1913−1919. (d) Distances for ferric nitrosyl porphyrins were calculated using the data for [Fe(TPP)(NO)(HO-*i*-C$_5$H$_{11}$)]$^+$ [18e] and [Fe(OEP)(NO)]-[ClO$_4$].[18f] (e) Yi, G. B.; Chen, L.; Khan, M. A.; Richter-Addo, G. B. *Inorg. Chem.* **1997**, *36*, 3876−3885. (f) Ellison, M. K.; Schulz, C. E.; Scheidt, W. R. *Inorg. Chem.* **2000**, *39*, 5102−5110.

(19) Ellison, M. K.; Schulz, C. E., Scheidt, W. R. *Inorg. Chem.* **2000**, *39*, 5102−5110

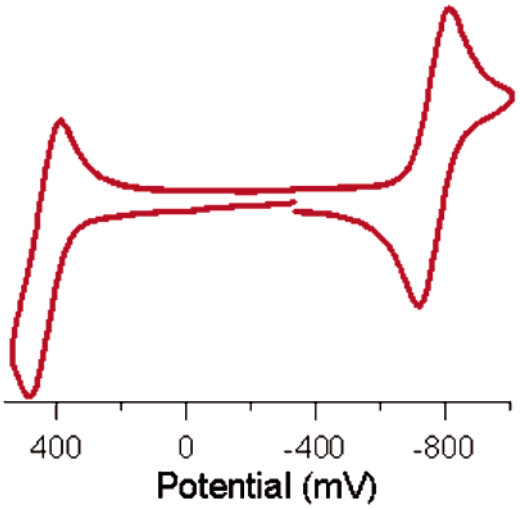


**Figure 4.** Cyclic voltammogram of Fe(TFPC)(NO) in $CH_2Cl_2$ containing 0.1 M TBAHP (referenced to $Fc^+/Fc$).

**Table 4.** Half-Wave Potentials (vs $Fc^+/Fc$) for the Oxidation and Reduction of Different $Fe(Ar_3C)(NO)$ Complexes in $CH_2Cl_2$ and 0.1 M TBAHP and the Nitrosyl Stretching Frequencies, $\nu_{NO}$ (thin film)

| $Fe(Ar_3C)(NO)$ | substituent constant[a] $\sum\sigma$ | oxidation $E_{1/2}$ (mV) | reduction $E_{1/2}$ (mV) | $\nu_{NO}$ ($cm^{-1}$) |
|---|---|---|---|---|
| Fe(TNPC)(NO) | 0.78 | 550 | −630 | 1772 |
| Fe(TBrPC)(NO) | 0.23 | 410 | −750 | 1767 |
| Fe(TFPC)(NO) | 0.06 | 450 | −780 | 1767 |
| Fe(TPC)(NO) | 0.00 | 390 | −810 | 1767 |
| Fe(TTC)(NO) | −0.17 | 340 | −850 | 1767 |
| Fe(TMOPC)(NO) | −0.27 | 340 | −870 | 1761 |
| Fe(OEC)(NO)[5b] | | 160 | −860 | 1767[b] |

[a] The sum of the Hammett substituent constants $\sigma$[20] for the three aryl rings, $\sum\sigma = 3\sigma$. [b] In $CH_2Cl_2$.

(NO) has been shown[5b] to demonstrate a rich electrochemistry with two reversible one-electron oxidations and one chemically irreversible oxidation, as well as two one-electron reductions, and a similar pattern was seen for representative $Fe(Ar_3C)(NO)$ complexes;[1] however, the present study focused simply on the first oxidation and reduction waves of the latter. Ferrocene was used as the internal standard. The representative voltammogram for Fe(TFPC)(NO) (ferrocene wave omitted for clarity) shows a reversible reduction at $E_{1/2} = -780$ mV and a reversible oxidation at 450 mV (both vs $Fc^+/Fc$), both with peak to peak separations, $\Delta E_p = |E_{pc} - E_{pa}|$, smaller than the ferrocene standard (75 and 56 mV, respectively, vs 100 mV for $Fc^+/Fc$). Similar behavior was seen for each $Fe(Ar_3C)(NO)$ complex, and the half wave potentials determined in this manner are listed in Table 4. In each case, the anodic to cathodic peak current ratios, $i_{ca}/i_{pa}$, are close to unity at a scan rate of 100 mV/s. This indicates that the electrochemical processes are reversible one-electron transfers and suggests that the NO axial ligand remains coordinated to the iron after both reduction and oxidation. A similar observation has been reported for Fe(OEC)(NO).[5b]

Figure 5 is a graphical representation of the $E_{1/2}$ values for the first oxidation and reduction waves of the $Fe(Ar_3C)$-(NO) complexes plotted as a function of the Hammett constants for the aryl ring substituents. As the substituents become more electron-donating, the half-cell potentials for both oxidation and reduction of $Fe(Ar_3C)(NO)$ predictably shift

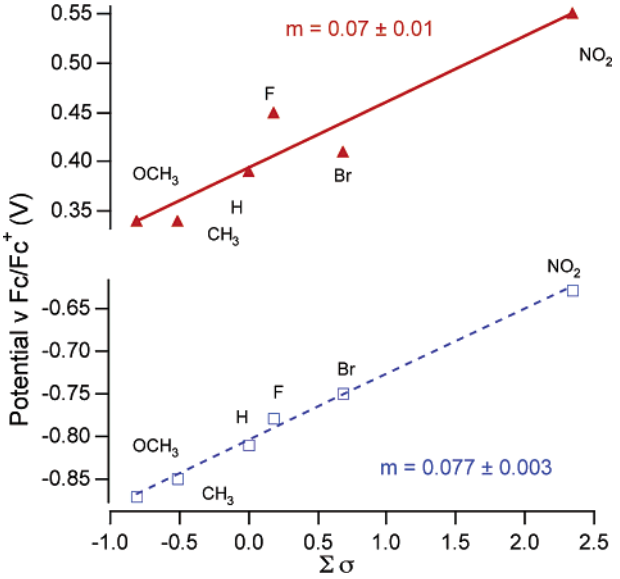


**Figure 5.** Plots of the half-wave potentials for $Fe(Ar_3C)(NO)^+/Fe(Ar_3C)$-(NO) (triangles) and $Fe(Ar_3C)(NO)/Fe(Ar_3C)(NO)^-$ (squares) couples against the summed Hammett substituent constant $\sum\sigma = 3\sigma$.

to more negative potentials. Both sets of data display linear relationships to the substituent constants, although the correlation is poorer (±14%) for oxidation than for reduction (±4%). Furthermore, comparison of the two plots reveals that, within experimental uncertainty, the slopes are the same, giving the respective correlations: $E_{1/2}$(ox) (in mV) = (70 ± 10)(3$\sigma$) + 390 and $E_{1/2}$(red) (in mV) = (77 ± 3)(3$\sigma$) − 810.

Similar correlations have been reported for two other series of corrolate complexes, $Co(Ar_3C)(PPh_3)$[21] and $Cu(Ar_3C)$.[22] For the former, the slope of the first reversible oxidation potential versus 3$\sigma$ is 57 mV; however, the first reduction showed irreversible behavior because of subsequent labilization of the phosphine. For the latter, the slope of the first oxidation potential versus 3$\sigma$ is 95 mV (or 56 mV when the pyrrole hydrogens are substituted with bromines) and the slope of first reduction potential versus 3$\sigma$ is 68 mV (86 mV for the perbromo pyrroles).

As noted above, the cyclic voltammetry of Fe(OEC)(NO) has been described by Kadish et al.,[5b] who assigned the locale of the first reduction to the metal center to give a species designated as the $[Fe^{II}(OEC)(NO)]^-$ anion and supported that assignment with in situ UV−vis, IR, and EPR spectroscopy. Particularly notable was the shift in the $\nu_{NO}$ band from 1767 $cm^{-1}$ in Fe(OEC)(NO) to 1585 $cm^{-1}$ in the one-electron reduction product. The reversible one-electron oxidation of the same material to give the $[Fe(OEC)(NO)]^+$ cation was interpreted based on IR ($\nu_{NO}$ = 1815 $cm^{-1}$) and EPR studies in terms of corrolate ligand oxidation to give an $Fe^{III}(\cdot C^{2-})(NO)$ species. The latter species was isolated as a perchlorate salt and characterized by X-ray crystallography.

These assignments for the localization of the one-electron oxidation and reduction are supported by DFT calculations

(20) Hansch, C.; Leo, A.; Taft, R. W. *Chem. Rev.* **1991**, *91*, 165−195.
(21) Adamian, V. A.; D'Souza, F.; Licoccia, S.; Di Vona, M. L.; Tassoni, E.; Paolesse, R.; Boschi, T.; Kadish, K. M. *Inorg. Chem.* **1995**, *34*, 532−540.
(22) Wasbotten, I. H.; Wondimagegn, T.; Ghosh, A. *J. Am. Chem. Soc.* **2002**, *124*, 8104−8116.

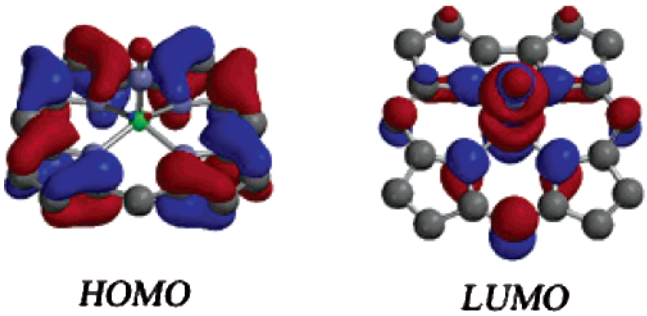


**Figure 6.** Contour diagrams for the HOMO and LUMO of Fe(C)(NO). The analogous diagram for HOMO−1 is shown in the Supporting Information.

(details in the Experimental Section and in the Supporting Information) of the simple unadorned corrole complex Fe(C)(NO). These showed the LUMO to be largely localized at the metal nitrosyl. The HOMO is primarily a $\pi$ MO of the corrole ring (Figure 6) in agreement with earlier calculations by Ghosh et al. for a Ga(III) corrolate.[23] In this context, the similarity in the slopes of the plots shown in Figure 5 is puzzling, since this would suggest that both the reduction and oxidation are localized similarly for the Fe(Ar$_3$)(NO) analogues. Qualitative examination of the HOMO and LUMO indicates that the former is delocalized over the four pyrolle rings with nodes at the meso carbons where the aryl groups are bound to the corrolate ring of $Ar_3C^{3-}$. In contrast, although the LUMO is mostly metal−NO antibonding in character, there is a moderate contribution from the ring $\pi$ orbitals located on the mesocarbons. In this context, it may be possible that the aryl ring substituents have similar quantitative effects on the two orbitals, the former largely by inductive effects, the latter by modest $\pi$ interactions via the meso carbons.

**IR Spectra.** Another effect of the trianionic charge of the corrolate ligand is indicated by the NO stretching frequency of the Fe(C)(NO) complexes, which is consistently lower than that seen for Fe(III) porphyrin complexes but higher than that for the Fe(II) porphyrin analogues (Tables 3 and 4). The $\nu_{NO}$ values are relatively insensitive to the aromatic ring substituents of various Fe(Ar$_3$C)(NO) complexes, although the general trend follows the electronic nature of the substituents, and the strongly electron-withdrawing pentafluorophenyl ring[24] does shift $\nu_{NO}$ ~30 cm$^{-1}$ to higher frequency.

**Flash Photolysis Studies.** The optical absorption spectra of the various Fe(Ar$_3$C)(NO) complexes in toluene solutions each display a broad, very strong band with a $\lambda_{max}$ in the range of 379−416 nm (extinction coefficients nearly $10^5$ M$^{-1}$ cm$^{-1}$) and another band in the range of 532−541 nm, about a factor of 8 less intense. These can be assigned to $\pi\pi^*$ transitions largely localized on the corrole macrocycle and are analogous to the Soret and Q-bands seen in the optical spectra of porphyrinato complexes.[23,25] The solutions of Fe(Ar$_3$C)(NO) proved to be quite stable, even when aerated, and there were no observable changes in their optical spectra when deaerated by entraining the solutions with argon or by subjecting them to a vacuum. Thus, spontaneous NO dissociation must be very slow, and the solutions are more stable than analogous nitrosyl complexes of ferrous or ferric porphyrinato.

As we have reported,[16] flash photolysis of toluene solutions of Fe(TNPC)(NO) using the excitation wavelengths ($\lambda_{ex}$) of 355 or 532 nm leads to transient bleaching of bands corresponding to the parent compound and to the appearance of strong transient absorbances. A rough estimate of the quantum yield of NO labilization suggests a value in the range of 0.5−1.0.[26] These absorption changes underwent rapid [NO]-dependent decay back to the original spectra. Although we did not succeed in preparing an analytically pure sample of the NO-free complex Fe(TNPC), comparing the optical spectra for Fe(TNPC) solutions prepared in situ with the transient spectra obtained by flash photolysis of Fe(TNPC)(NO) in toluene offered strong evidence that flash photolysis leads to reversible NO labilization (eq 1). Similar flash photolysis-induced NO dissociation has been described for nitrosyl complexes of iron(II) and iron(III) porphyrinato analogues in solution.[12a,12g,13a−c]

$$\mathrm{Fe(TNPC)(NO)} \underset{k_{NO}[\mathrm{NO}]}{\overset{h\nu}{\rightleftharpoons}} \mathrm{Fe^{III}(TNPC)} + \mathrm{NO} \qquad (1)$$

Each of the Fe(Ar$_3$C)(NO) complexes studied showed similar transient spectral changes upon laser flash photolysis. In the presence of excess NO, the transient absorbances (and bleaches of parent spectra) decayed via first-order kinetics from which fits of $\Delta$abs versus time profiles to an exponential function gave the rate constants, $k_{obs}$, for each set of conditions. Plots of $k_{obs}$ versus [NO] (0.5−3.0 mM) were linear with $y$ intercepts near zero (Figure 7), consistent with the rate law expressed in eq 2. The slopes of such linear plots are the second-order recombination rate constants, $k_{NO}$. The values of $k_{NO}$ determined by flash photolysis of various Fe(Ar$_3$C)(NO) solutions are summarized in Table 5.

$$\left(\frac{\mathrm{d[Fe(Ar_3C)]}}{\mathrm{d}t}\right) = -k_{NO}[\mathrm{NO}][\mathrm{Fe(Ar_3C)}] \qquad (2)$$

(23) Ghosh, A.; Wondimagegn, T.; Parusel, A. B. *J. Am. Chem. Soc.* **2000**, *122*, 5100−5104.
(24) Wehman, P.; Borst, L.; Kamer, P. C. J.; van Leeuwen, P. W. N. M. *J. Mol. Catal. A* **1996**, *112*, 23−36.
(25) Gouterman, M. In *The Porphyrins*; Dolphin D., Ed.; Academic Press: New York, 1978; Vol. III, Chapter 1.

(26) The quantum yield estimate was made as follows. The energy of the laser pulse and the absorbance of the solution at the laser excitation wavelength (532 nm) give the total number of photons, $N_q$, absorbed by the solution. This excitation is contained within a cylinder of solution defined by the diameter of the laser pulse (6 mm) and by the cell path length with a volume, $V_p$. The detection light beam is perpendicular to the cylinder at approximately the midway point and is much smaller in diameter, so the actual volume of photolyzed solution monitored, $V_m$, is a small fraction of $V_p$. The number of photons absorbed by this volume of solution is estimated as $N_q(p) = N_q \times (V_m/V_p)$. The absorbance change measured in $V_m$ is used to calculate the number of molecules, $N_m$, photochemically converted inside $V_m$, and so the quantum yield, $\Phi$, is estimated as $N_m/N_q(p)$. Among the likely errors in this estimate is the assumption that the light is absorbed uniformly by a cylinder of solution, since the laser pulse has a Gaussian radial distribution hence is likely to be more intense in the center, where the monitoring pulse was located. This would tend to underestimate $N_q(p)$ and thus overestimate $\Phi$. Despite this, the qualitative observation of relatively strong transient absorption changes suggests a moderately high value of $\Phi$.

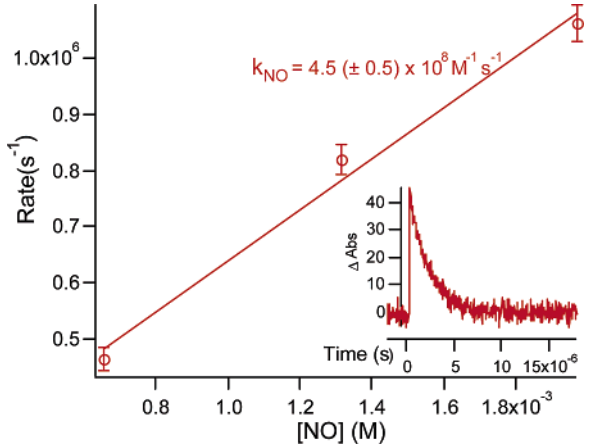


**Figure 7.** A plot of the $k_{obs}$ values resulting from the flash photolysis of Fe(TMOPC)(NO) in toluene solutions vs [NO]. The calculated best fit line depicted is the second-order rate constant. Inset: Transient absorbance trace at 435 nm upon flash photolysis.

**Table 5.** Recombination Rate Constants, $k_{NO}$, for the Reaction of NO with $Fe^{III}(Ar_3C)$ in 295 K in Toluene Solutions and a Comparison to Certain Iron Porphyrinate Analogs

| $Fe^{III}(Ar_3C)$ | $k_{NO}$ ($M^{-1}$ $s^{-1}$) |
|---|---|
| $Fe^{III}$(TNPC)[a] | $(9.0 \pm 0.5) \times 10^8$ |
| $Fe^{III}$(TTC)[a] | $(5.9 \pm 0.1) \times 10^8$ |
| $Fe^{III}$(TPC)[a] | $(5.8 \pm 0.9) \times 10^8$ |
| $Fe^{III}$(TMOPC) | $(4.5 \pm 0.5) \times 10^8$ |
| $Fe^{III}$($TF_5$PC) | $(4.0 \pm 0.9) \times 10^8$ |
| $Fe^{III}$(TFPC) | $(1.6 \pm 0.4) \times 10^8$ |
| $Fe^{III}$(TBrPC) | $(1.3 \pm 0.1) \times 10^8$ |
| $Fe^{II}$(TPP)[b] | $5.2 \times 10^9$ |
| $Fe^{III}$(TPP)($NO_2$)[c] | $4.2 \times 10^5$ |

[a] Ref 16. [b] In benzene at ~295 K, ref 28. [c] $T = 298$ K, ref 27.

The $k_{NO}$ values obtained with $Fe(Ar_3C)$ ($(1.3-9) \times 10^8$ $M^{-1}$ $s^{-1}$) are generally several orders of magnitude larger than that ($4 \times 10^5$ $M^{-1}$ $s^{-1}$) recorded for the ferric tetraphenylporphyrinato complex Fe(TPP)($NO_2$) (eq 3) under analogous conditions.[27] The rates for $Fe(Ar_3C)$ are instead much closer to that for the NO reaction with the ferrous complex Fe(TPP) ($k_{NO} = 5.2 \times 10^9$ $M^{-1}$ $s^{-1}$ in benzene) following flash photolysis of Fe(TPP)(NO).[28] Furthermore, since spontaneous NO dissociation of $Fe(Ar_3C)(NO)$ is very slow ($k_{off} < 10^{-3}$, estimated), the equilibrium constants, $K_{NO} = k_{NO}/k_{off}$, must be very large ($>10^{11}$ $M^{-1}$), a property again much more similar to the ferro-heme than the ferri-heme models.[4,5] The high reactivity of $Fe(Ar_3C)$ is only slightly moderated by adding coordinating solvents such as tetrahydrofuran, acetonitrile, or even pyridine.[16] This has been rationalized in terms of this intermediate remaining (no more than) 5-coordinate even when substantial concentrations of these ligands are present, leaving a site accessible to reaction with NO. The reluctance of $Fe(Ar_3C)$ to bind such Lewis bases as hexacoordinate complexes can be attributed to the strong electron donor character of the $Ar_3C^{3-}$ ligand.

$$\text{Fe(TPP)(NO)(NO}_2\text{)} \underset{k_{NO}[NO]}{\overset{h\nu,\ k_{off}}{\rightleftharpoons}} \text{Fe}^{III}\text{(TPP)(NO}_2\text{)} + \text{NO} \qquad (3)$$

Comparison of the $k_{NO}$ values listed in Table 5 shows no obvious trend with the Hammett $\sigma$ constants for the aromatic substituents listed in Table 4. We had anticipated that since the reaction of $Fe(Ar_3C)$ with NO represents (at least formally) a reduction of the Fe(III) center,[14] the rates might be faster for electron-withdrawing substituents. However, while the $k_{NO}$ values are sensitive to the substituents, there is no obvious correlation to the electronic properties reflected by their $\sigma$'s. In an earlier discussion,[16] we attributed the fast recombination rates of $Fe(Ar_3C)$ complexes to the low Lewis acidities noted above and to the role of quartet spin states which result in a half-occupied $\sigma^*$ $d_{z^2}$ iron orbital. In the absence of a more obvious explanation, we speculate that the 3/2 spin contribution to the electronic ground state of $Fe(Ar_3C)$ at ambient temperature may vary in a nonlinear relationship to the substituent Hammett $\sigma$ values. Notably, we have also measured $k_{NO}$'s for a series of ferric TPP derivatives $Fe(Ar_4P)(NO_2)$ (generated by the flash photolysis of $Fe(Ar_4P)(NO_2)(NO)$ in toluene). These fall into the range of $(2.0-4.3) \times 10^5$ $M^{-1}$ $s^{-1}$ (298 K), but again, they show little correlation with the electron-withdrawing or -donating character of the aromatic ring substituents.[29]

**Acknowledgment.** This research was supported by the National Science Foundation (CHE-0352650). We thank Professor M. Emrah Kilinc, NATO Fellow from Ege University, Faculty of Pharmacy, Izmir, Turkey, and Professor Kiyoshi Tsuge, visitor from Hokkaido University, Japan, who provided valuable assistance with electrochemical measurements.

**Supporting Information Available:** Cell packing diagrams for two crystal structures as well as tables with listings of complete structure refinement details, bond lengths and angles, anisotropic displacement parameters for non-hydrogen atoms, and hydrogen coordinates and isotropic displacement parameters. Also a table of computational results. This material is available free of charge via the Internet at http://pubs.acs.org.

IC051956J

(27) Lim, M. D.; Lorkovic, I. M.; Wedeking, K.; Zanella, A. W.; Works, C. F.; Massick, S. M.; Ford, P. C. *J. Am. Chem. Soc.* **2002**, *124*, 9737−9743.
(28) Hoshino, M.; Kogure, M. *J. Phys. Chem.* **1989**, *93*, 5478−5484.
(29) (a) Lim, M. D. Ph.D. Dissertation, University of California, Santa Barbara, 2004. (b) Lim, M. D., Patterson, J. C.; Kurtikyan, T.; Ford, P. C. manuscript in preparation.